Chapter 4
Recent Advances in Electrocatalysis of Formic Acid Oxidation

Cynthia Ann Rice, Akshay Bauskar, and Peter G. Pickup

Abstract Direct formic acid fuel cells offer an alternative power source for portable power devices. They are currently limited by unsustainable anode catalyst activity, due to accumulation of reaction intermediate surface poisons. Advanced electrocatalysts are sought to exclusively promote the direct dehydrogenation pathway. Combination and structure of bimetallic catalysts have been found to enhance the direct pathway by either an electronic or steric mechanism that promotes formic acid adsorption to the catalyst surface in the CH-down orientation. Catalyst supports have been shown to favorably impact activity through either enhanced dispersion, electronic, or atomic structure effects.

4.1 Introduction

Fundamental anode catalyst research is imperative for improved direct formic acid fuel cell (DFAFC) performance and stability; such that an intimate understanding of the interplay between structural, morphological, and physicochemical properties is needed. The primary base catalysts found to be active for formic acid electrooxidation are either platinum (Pt) or palladium (Pd). The cyclic voltammograms in Fig. 4.1 compare the activity of carbon-supported Pt to Pd towards formic acid electrooxidation. The anodic (forward) scan, relevant to DFAFC performance, is relatively inactive on Pt/C until the applied potential

C.A. Rice (✉) • A. Bauskar
The Center for Manufacturing Research, Department of Chemical Engineering, Tennessee Tech University, Cookeville, TN 38505, USA
e-mail: criceyork@tntech.edu

P.G. Pickup (✉)
Chemistry Department, Memorial University, St. John's, NL, Canada A1B 3X7,
e-mail: ppickup@mun.ca

M. Shao (ed.), *Electrocatalysis in Fuel Cells*, Lecture Notes in Energy 9,
DOI 10.1007/978-1-4471-4911-8_4,

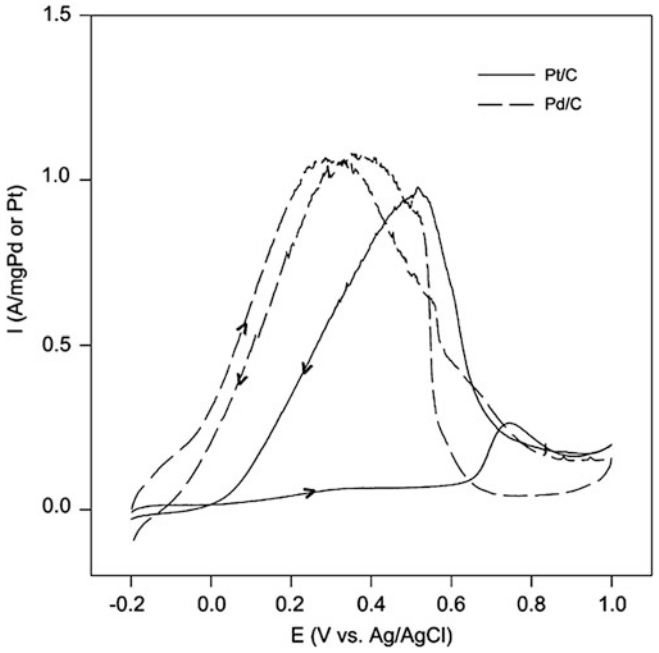

Fig. 4.1 Cyclic voltammograms on Pt(4 nm)/C and Pd(5 nm)/C in 3 M formic acid and 1 M H_2SO_4 at 10 mV s^{-1} [101]

exceeds 0.8 V vs. RHE (ca. 0.6 V vs. Ag/AgCl), due to the dominance of the indirect dehydration pathway [(3.2) in Chap. 3]. Conversely, on the Pd/C catalyst, large currents are immediately observed at very low potentials, because initially the reaction on a Pd surface is almost exclusively by the nonpoison-forming direct dehydrogenation pathway [(3.1) in Chap. 3].

The reason for Pd's enhanced activity is due to the breakage of the H–COOH bond by adsorption in the CH-down orientation, while Pt promotes the breakage of the HC(O)–OH bond by adsorption in the CH-up orientation [1–4]. Although Pd is significantly more active than Pt, it lacks sustained high performance. Pd has the propensity to generate intermediate species that slowly stifle the direct pathway [5–8], as well as to lose active area due to Pd dissolution in an acid environment [9, 10]. Research and development activities for advanced anode catalysts for DFAFCs are driven by the need for increased activity, sustained activity during long-term operation of the cell, and reduced cost. To that end secondary metals have been incorporated into the Pt- or Pd-based catalyst. Table 4.1 enumerates several precious and non-precious metals that have been investigated in combination with either Pt or Pd [11]. Group III elements have a distinct cost advantage over Groups I and II. Since none of these have completely eliminated the activity loss for Pd-based (Pt-free) catalysts, and some (notably Bi, Pb, and Sb) result in greatly enhanced and stable performances for Pt-based catalysts, there is substantial activity in the further

Table 4.1 Groupings of secondary metals having been incorporated into Pt- or Pd-based anode catalysts for formic acid electrooxidation (adapted from [11])

	Elements	Classification	Remarks
Group I	Au, Ir, Pd, Pt, Ru	Precious metals	Enhancement of Pt
Group II	Cr, Cu, Fe, Mo, Nb, V	Transition non-precious metals	Thermodynamic properties
Group III	Bi, Pb, Sb, Sn	Post-transition metals	Reduced cost

development of both of these types of catalyst. In the case of Pt-based catalysts, the focus is now on the development of supported, low Pt loading catalysts (e.g., Pt on carbon; Pt/C), and the search for novel support materials that increase activity [12, 13].

Catalyst activity towards formic acid electrooxidation is strongly influenced by preparation method and nanoparticle size. As discussed in the previous chapter, the optimal sizes for Pt/C and Pd/C are 4 nm and 5.2–6.5 nm, as determined by Park et al. [14] and Zhou et al. [15], respectively. This chapter is segregated into two sections: bimetallic catalysts and catalyst supports. The section on bimetallic catalysts is subdivided into adatoms, alloys, and intermetallics.

4.2 Bimetallic Catalysts

The goal of the addition of a secondary metal is to enhance activity and/or stability. Adatoms are adsorbed onto preformed catalyst surfaces. While for both alloys and intermetallics, the composition of a base metal (typically Pt or Pd) is altered by the addition of a secondary metal as part of the preparation procedure. The key difference between the two is that alloys are characterized by a random mixture of at least two metallic solid solution phases, while intermetallics are defined as ordered solid solution phases with fixed stoichiometry and identical atomic unit cells. The resulting intermetallics have uniform geometries, resulting in control of the electronic environment [16].

4.2.1 Adatoms

A common method for improving formic acid electrooxidation activity is through the incorporation of foreign adatoms in sub- or monolayer coverages onto metal electrocatalyst surfaces (substrates). Adatoms are usually deposited onto the metal surface either by under potential deposition (UPD) or by irreversible adsorption [17]. The two dominant reaction enhancement mechanisms for the direct dehydrogenation pathway, as described in Sect. 3.3 of the previous chapter for formic acid electrooxidation, are the third-body and electronic effects. The type of enhancement mechanism due to adatom addition is dependent on the substrate/adatom

Table 4.2 Activity of Pt(111) adatom electrodes, from anodic portion of cyclic voltammogram in 0.25 M formic acid and 0.5 M H_2SO_4 (except Te in 0.1 M formic acid) at 50 mV s^{-1}

Adatom on Pt(111)	Optimal coverage (θ)	I at 0.4 V (mA cm^{-2})	Anodic peak E (V)	Anodic peak I (mA cm^{-2})	Primary enhancement mechanism	References
Pure	n/a	0.57	0.53	1.12		[20]
Se	0.28	0.1	0.71	3.4	Third body	[39]
As	0.31	0.35	0.54	4.6	Electronic	[35]
Te	0.3	0.9	0.75	6.2	Electronic	[38]
Pd	0.28	1.5	0.50	2	Third body	[5]
Pd/Pt(100)	0.7	14	0.22	55	Electronic	[5]
Bi	0.82	15.5	0.495	35	Electronic	[20]

Potentials (E) vs. RHE and current (I)

configuration and/or electronic interaction. Results in the literature suggest that both effects promote the adsorption of formic acid in the CH-down direction which is a predetermining factor for the direct reaction pathway [2–4].

The most commonly investigated substrates have been Pt and Pd, ranging from well-defined single-crystal surfaces to nanoparticles. Bismuth (Bi) has been the most extensively tested adatom [18–28]. Other adatoms that have also exhibited performance enhancements are lead (Pb) [29–31], antimony (Sb) [2, 22, 29, 32, 33], arsenic (As) [34, 35], gold (Au) [36], tellurium (Te) [37, 38], selenium (Se) [39], ruthenium (Ru) [40], and palladium (Pd) [5, 40, 41]. Researchers have seen that, for the various adatoms, higher coverages promote the direct reaction pathway.

4.2.1.1 Single-Crystal Surfaces

To illustrate the primary effects of adatom addition, single-crystal electrodes are discussed here. Feliu and Herrero have extensively studied formic acid electrooxidation on Pt single-crystal substrates modified with an array of various adatoms. They have established a connection between the electronegativity of the adatoms in relation to Pt and the type of active enhancement mechanism incurred as a function of adatom coverage [42]. Their results support inhibition of the indirect pathway on Pt(111) terraces and they have demonstrated that CO_{ads} formation occurs at step and defect sites. For Pt(111) substrates decorated with electropositive adatoms, such as Bi, Pb, Sb, and Te, the electronic enhancement is extended to the second or third Pt atom shell from the adatom. While for electronegative adatoms, in respect to Pt, the third-body effect dominates with increased coverages, such as S and Se.

Table 4.2 highlights the extensive work done in Feliu's group on adatom-decorated Pt(111) substrates—specifically Se, As, Te, Pd, and Bi. Cyclic voltammogram results are compared for the first forward sweep in 0.25 M formic acid and 0.5 M H_2SO_4 at 50 mV s^{-1} vs. RHE. Two distinct phenomena can be differentiated based on their results: (a) formic acid electrooxidation activity at low overpotentials and (b) the

amount of surface poison. For Se, As, and Te, the optimal coverage was found to be around 0.3. Coverages in excess of 0.3 for these adatoms resulted in a decrease in overall performance. We have selected a potential of 0.4 V to evaluate fuel cell relevant anode catalyst activity, where the indirect dehydration pathway does not significantly contribute to the current density. At 0.4 V for these three modifiers, an increase in current density over the Pt(111) baseline was observed only for Te, while for Se and As the current density decreased. The peak current density with these modifiers was observed above 0.5 V and higher than that of the Pt(111) baseline. To evaluate the extent of poison formation as a function of adatom coverage, the electrodes were held at 0.1 V for an extended period of time in formic acid containing electrolyte, after which the solution was exchanged with pure electrolyte and a cyclic voltammogram was initiated to strip off CO_{ads}. Formic acid dissociation to CO_{ads} was found to only occur on the Pt substrate, thus the adatoms do not directly participate in the reaction. The CO_{ads} on Se-decorated surfaces decreased linearly with increasing adatom coverages, consistence with a primarily third-body effect, i.e., higher coverages are required to induce steric inhibition of the CH-up adsorption in the indirect pathway [43]. Conversely Te follows the trend of an electronic effect promoting CH-down adsorption for the direct pathway up to 6–8 Pt atom away from the adatom. For As-decorated surfaces, the magnitude of the electronic effect is diminished by adatom desorption at open-circuit potentials in the presence of formic acid, as is also found for Sn- and Pb-decorated Pt surfaces [42].

For Pd- and Bi-decorated surfaces, higher coverages resulted in enhanced performances. For $\theta_{Pd} = 0.28$, the observed current density at 0.4 V was nearly three times that of the Pt(111) baseline, but there was only marginal improvement at the peak potential which was only slightly lower than at pure Pt. In comparison, Bi has an optimal coverage at 0.82 with a 27 times increase in activity at 0.4 V relative to Pt. The CO_{ads} stripping coverage dependence followed the linear decrease characteristic of a third-body effect for Pd on Pt(111) (albeit at a steeper slope than Sb), while Bi produced an exponential decrease consistent with an electronic enhancement. The optimal coverage of Pd increased to 0.7 on Pt(110) and the current density at 0.4 V was comparable to that of the optimal Bi-modified surface. The key difference for the Pd/Pt(100) combination is that the maximum peak potential is shifted to 0.22 V with a current density of 55 mA cm^{-2}.

4.2.1.2 Nanoparticles

The driving force for small nanoparticle catalysts is reduced cost by minimizing inactive non-surface atoms, which is the basis of most low Pt approaches. Yu and Pickup investigated the coverage dependence of Pb and Sb on commercial 40 wt% Pt supported on carbon in situ in a formic acid/O_2 fuel cell [29]. They found optimal coverages of 0.7 for both types of adatoms. The performance of both PtSb/C and PtPb/C far exceeded that of Pt/C. After nearly a 2 h hold at 0.6 V under fuel cell operation, the performance increase over Pt/C was 15- and 12.8-fold, respectively. Figure 4.2 is a comparison of fuel cell performance at 0.6 V as a function of adatom

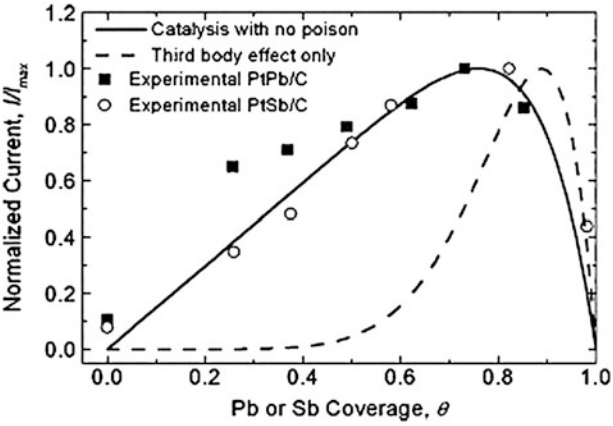

Fig. 4.2 Plot of direct formic acid fuel cell performance at 0.6 V for Pt/C anodes as a function of Pb and Sb adatom coverages. The experimental data is compared to the two formic acid electrooxidation models proposed by Leiva: (*solid line*) electronic enhancement and (*dashed line*) third-body effect [29]

coverage. This cell voltage corresponds to a relatively low anode overpotential in a region where the direct pathway would exclusively contribute to the measured power density. The results are compared to the model developed by Leiva et al. [44] for the two dominant formic acid electrooxidation enhancement mechanisms—third body (dashed line) vs. electronic (solid line). The results follow the trend line for an electronic enhancement, whereas Leiva et al. [44] reported that increasing the coverage of Sb on a Pt(100) single crystal displayed a third-body enhancement effect (Fig. 3.7 in Chap. 3). The divergence in dominant enhancement mechanism for an Sb-decorated Pt substrate is potentially twofold: (a) the facet structure of the Pt substrate and/or (b) the dispersion of the Sb. The Pt/C nanoparticles used in Yu and Pickup's work were 2.5 nm in diameter, possessing typical cuboctahedral features depicted in Fig. 4.3 with fractal Pt(111) and Pt(110) contiguous terraces and an abundance of low coordination corners and edges. Also, their decoration method was via chemical deposition as opposed to under potential deposition, which may produce an alternative more active adatom dispersion on a per Pt basis, in comparison to that prepared by Lee et al. by UPD [33].

Wieckowski's group has studied formic acid electrooxidation on Pt nanoparticles decorated with controlled amounts of Pd and Pd+Ru adatoms [41]. They reported two orders of magnitude increase in the reactivity of the Pd-decorated catalyst compared to pure Pt towards formic acid oxidation. Also, it was concluded that the impact of CO_{ads} on the Pt/Pd catalyst through the dual pathway mechanism is much lower even though the potential required to remove CO_{ads} from the surface was the highest.

Bi et al. boosted the performance of Pt nanoparticles towards formic acid electrooxidation by depositing sub-monolayer Au clusters [36]. The modified Pt nanoparticles exhibited a 23-fold increase in specific activity. This enhancement in

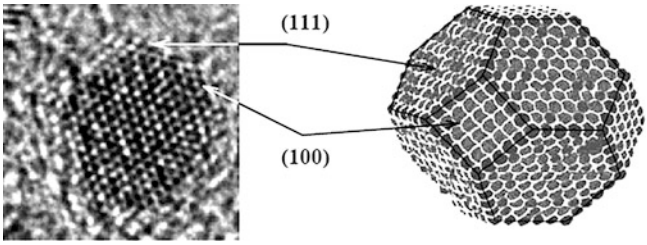

Fig. 4.3 (*Left*) High-resolution TEM image of a Pt/C nanoparticle. (*Right*) Pictorial proposed representation of the cuboctahedral Pt nanoparticle, with Pt(111)- and Pt(100)-faceted terraces identified [102]

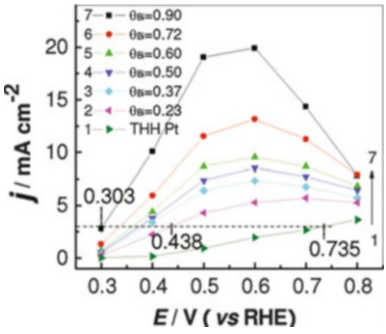

Fig. 4.4 Current density at 60 s after transient potential holds on 81 nm tetrahexahedral (THH) Pt nanoparticles as a function of Bi coverage. The dashed line is for a 3 mA cm^{-2} performance target [18]

catalytic activity was attributed to the inhibition of the indirect reaction pathway by the third-body effect.

Bismuth has attracted significant interest as a Pt/C modifier for formic acid electrooxidation [21, 24, 26, 27]. A wide range of stable and well-characterized electrode surfaces modified by irreversible Bi adatom adsorption on Pt have been reported in the literature for a range of Bi coverages (θ). Chen et al. have explored Bi adatom decoration on 81 nm tetrahexahedral Pt nanoparticles that while composed of (100) and (110) facets that are the least active for formic acid electrooxidation, they are bound by {730} and vicinal high-index facets that are extremely active [18]. They have measured current densities of 10 mA cm^{-2} for Bi coverages up to 0.9 at 0.4 V in 0.25 M formic acid and 0.5 M H_2SO_4 solution; see Fig. 4.4. They also showed steady-state activity at 0.3 V of 2.8 mA cm^{-2} after 1 min vs. 0.0003 mA cm^{-2} for the non-modified Pt baseline.

Kim et al. [24] reported a detailed analysis on formic acid electrooxidation on 3 nm Pt/C modified by irreversible adsorption of Bi. They ascribed the enhancement in catalytic activity to promotion of the direct pathway, which is dependent on the oxidation state and coverage of the Bi. For Bi coverage on Pt above 0.54, the oxidation rate of formic acid increased by a factor of 8. The amounts of CO and

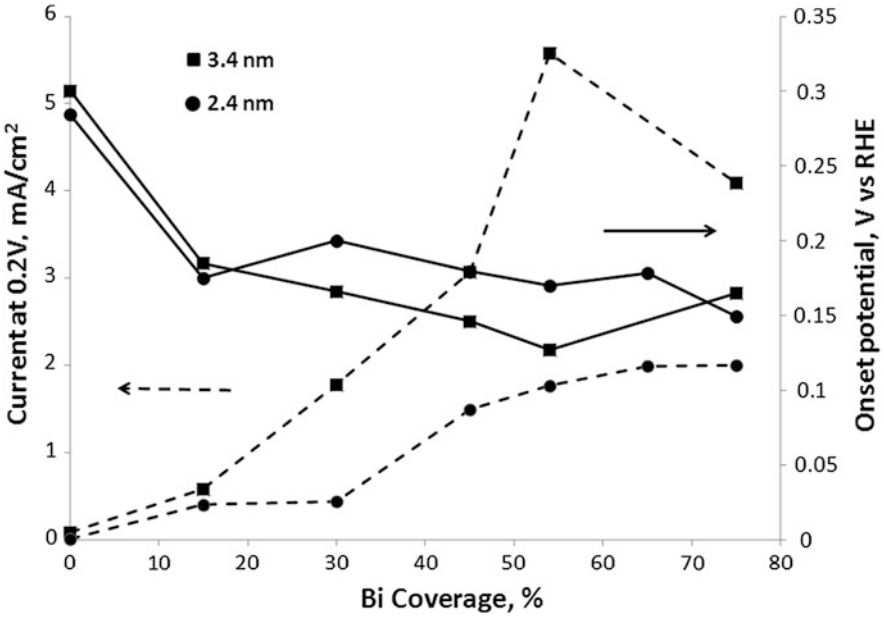

Fig. 4.5 Anodic current density acquired during a cyclic voltammogram at 0.2 V vs. RHE for 3.4 nm and 2.4 nm Pt/C as a function of Bi coverage, in 0.1 M formic acid and 0.1 M $HClO_4$. Onset potential for formic acid electrooxidation of Bi-modified Pt electrodes (unpublished work from Rice's group)

poison were proportional to Bi coverage with a negative slope indicating the blocking of Pt sites by Bi for CO adsorption thereby impeding the dehydration pathway predominantly by the third-body enhancement effect. At a θ_{Bi} of 0.75, the anodic current density at 0.55 V vs. RHE was around 4.5 mA cm^{-2} after a 33 min hold, demonstrating an eightfold increase over the Pt baseline.

Bauskar and Rice have recently investigated an alternative method of adsorbing adatoms onto Pt/C substrates using a solution surface potential method amenable to mass scale-up [28]. Figure 4.5 tracks the change in formic acid electrooxidation current at 0.2 V vs. RHE as a function of Bi coverage for two commercial Pt/C nanoparticle sizes (2.4 nm and 3.4 nm). The performance is compared on a specific surface area basis to limit undesirable mass activity effects. The larger nanoparticles exhibit higher per surface atom activity at Bi coverages above 0.15. The initial rise in activity of the 3.4 nm Pt/C with Bi coverages up to 0.45 is indicative of an electronic enhancement, while the jump at around 0.54 would suggest a coverage-dependent shift in the dominant enhancement mechanism to third body. In contrast the activity-coverage-dependent features of the 2.4 nm Pt/C lack strong characteristics of either mechanism. Onset potentials for the unmodified Pt/C nanoparticles are similar, although slightly less for the 2.4 nm than 3.4 nm particles. Upon adsorption of 0.15 of a layer of Bi, the onset potential drops by nearly 0.11 V for both nanoparticle sizes, from 0.3 V to less than 0.2 V. Subsequent increases in Bi coverage induce a

slight additional decrease in the onset potential to around 0.15 V. Similar studies on Bi-modified mesoporous platinum microelectrodes resulted in a 0.15 V lower onset potential with respect to an unmodified mesoporous platinum microelectrode [21].

Scale-up for mass production can also potentially be achieved by reductive chemical deposition of metals such as Bi [27], Pb [29], and Sb [29] onto preformed Pt/C. For Bi, it was found that optimum performance occurred at very low surface coverage (ca. 0.15), which is not consistent with the third body or electronic enhancement models that work with other Bi on Pt catalysts or Pt/C modified with Sb and Pb in the same way [27]. However, it is consistent with observations that a Bi coverage as low as 0.04 can suppress CO formation on Pt(111) [34, 42]. These observations highlight the sensitivity of the enhancement mechanism to the way in which adatoms are deposited on the Pt surface, as well as possible differences in the structures of the modified Pt particles.

4.2.2 Alloys

In keeping with the focus of this book, "A Non and Low Platinum Approach," we have elected to restrict our discussion of recent catalyst advances here to either carbon-supported Pt or non-Pt-containing alloyed catalysts. The interested reader is directed to the following papers and review articles [45] on unsupported Pt alloys: PtHg [46], PtCd [46], PtCu [47], PtTi [48], and PtFe/Au [49]. To reduce cost, the reduction in the relative amounts Pt and Pd is desirable while approaching or exceeding the initial activity of Pd.

Pt/C-based—The introduction of a second metal to Pt has resulted in performance increases in a number of cases. For carbon-supported lead (Pb) alloyed with Pt (PtPb/C) in a nearly 1:1 atomic ratio, Huang et al. showed that for a 5.9 nm average PtPb particle size the anodic performance increased 74-fold over commercial Pt/C at 0.4 V vs. RHE [50, 51]. Unfortunately, the magnitude of the initial enhancement was not maintained under chronoamperometric testing; within the first few seconds of the hold, there was a substantial decrease in performance and after holding for only 30 min the performance difference to that of Pt/C was less than threefold.

Obradovic et al. investigated two different PtAu/C preparation methods [52]. They observed a 39-fold increase in activity at 0.4 V vs. RHE for a PtAu-modified Au(18.3 nm)/C core over the Pt(2.5 nm)/C baseline. The performance enhancement was only transitory, resulting in a rapid loss in performance. Chen et al. synthesized a systematic series of Pt_xAu_{x-1}/C alloys with sizes ranging from 4.5 to 5.5 nm. For the 1:1 Pt to Au alloy ($Pt_{0.5}Au_{0.5}$/C) at 0.1 V vs. SCE (0.344 V vs. RHE), an 8.8-fold improvement was observed over Pt/C [53]. The activities of both catalysts decayed at similar rates, but after 30 min the $Pt_{0.5}Au_{0.5}$/C was able to maintain a 9.2-fold improvement.

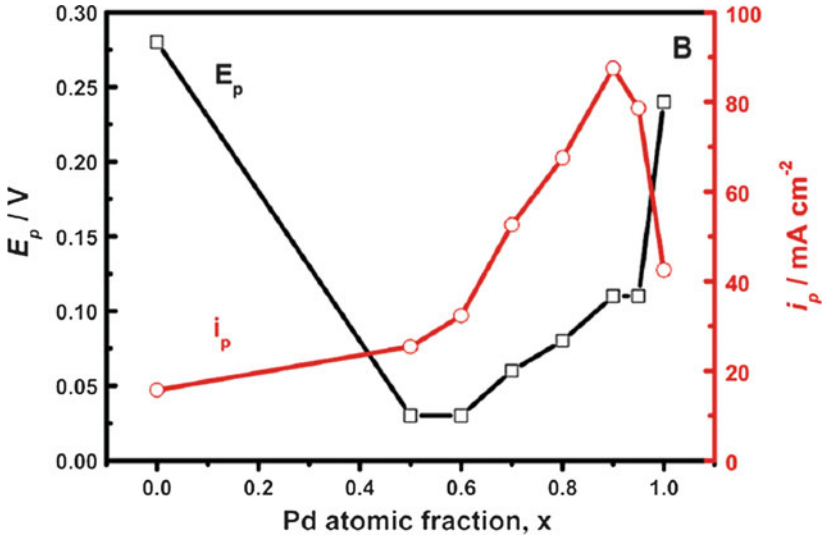

Fig. 4.6 Maximum anodic peak potential (E_p) vs. SCE (0.244 V vs. RHE) and peak current density (I_p) acquired during a cyclic voltammogram at 50 mV s^{-1} for Pd_xPt_{1-x}/C atomic fractions, in 0.5 M formic acid and 0.5 M H_2SO_4 [55]

Carbon-supported PtSb alloy catalysts have been shown to provide high and stable performances for formic oxidation in DFAFCs over 2 h periods [54]. Optimum performances were obtained for 1.8 nm particles with a 0.29 mol fraction of Sb.

Several groups have explored replacing a fraction of Pt with less expensive Pd [55–57]. Zhang et al. have systematically prepared and evaluate Pd_xPt_{1-x}/C, with atomic fractions of $x = 0.5$–1 for a narrow size distribution of 3.2–3.8 nm and compared their performances to Pt/C, as shown in Fig. 4.6 [55]. Pt/C was the least active in regard to peak potential (E_p) and peak current density (I_p). The lowest Pd content tested was $Pd_{0.5}Pt_{0.5}$/C, which resulted in a favorable 0.25 V decrease in anodic peak potential (E_p) with a slight increase in current density (I_p). As the Pd fraction was increased, E_p trended back towards the value for Pt, but I_p continued to increase, reaching a maximum for $Pd_{0.9}Pt_{0.1}$/C. For this composition, the current was 5.9- and 2.1-fold higher relative to Pt/C and Pd/C, respectively.

An attempt to produce PtBi alloy nanoparticles on carbon produced highly active catalysts for formic acid oxidation, although XRD showed no evidence of alloy formation [27]. Highest performances were obtained with a Bi:Pt mole ratio of just 0.07.

Pd/C-based—Metals, metalloids, and nonmetals have been alloyed with Pd in order to increase its activity and/or prevent or minimize its activity decay during formic acid oxidation. Increases in activity with boron (B) [58] and phosphorous (P) [59–61] have been attributed to a reduction in the 3d electron density and an increase

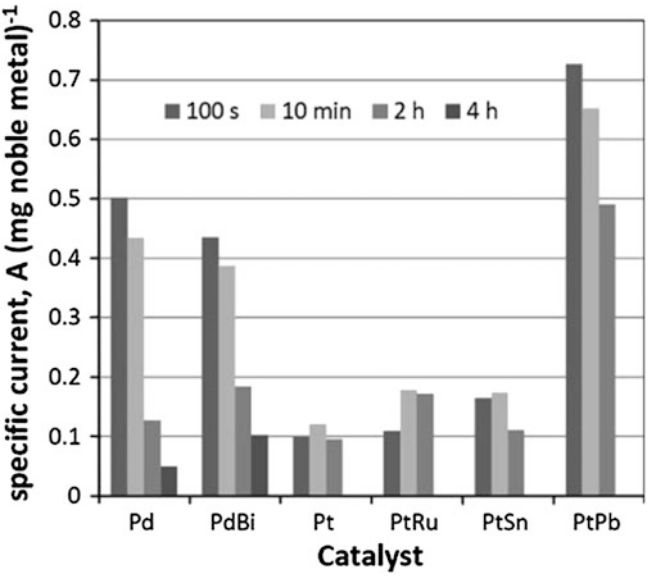

Fig. 4.7 Specific current acquired from DFAFC chronoamperometric holds at 0.3 V for selected catalyst combinations, 5 M formic acid at 0.2 ml min^{-1} and O_2 at 100 ml min^{-1} on the anode and cathode, respectively. Alloys—PdBi(4:1)/C and PtRu(1:1)/C. Adatoms—PtSn(8:1)/C and PtPb (8:1)/C [71]

in the percentage of metallic Pd [59]. The increases in activity were modest, between 1.3 and 1.9 times, while decay rates during potential holds were similar to those for unmodified Pd/C, albeit at higher current density values.

Several research groups have explored the addition of cobalt (Co) to Pd [62–66]. Wang et al. found that the addition of a third metal (iridium (Ir)) to a PdCo/C catalyst resulted in further enhanced activity [65]. At 0.294 V vs. RHE (0.05 V vs. SCE), the current density increases were 1.5- and 2.5-fold for Pd_2Co/C and Pd_4Co_2Ir/C, respectively, over that of Pd/C. The stabilities of the catalysts were evaluated at 0.344 V vs. RHE (0.10 V vs. SCE) and after a 16.7 min hold the Pd_4Co_2Ir/C current density was 18.4 times that of Pd/C, however, with a continued decreasing slope.

Tin (Sn)/Pd carbon-supported alloys have shown enhanced activity and stability [67–71]. Although Sn is completely inactive towards formic acid electrooxidation, a decrease in the 3d electronic density has been observed. An atomic ratio of Sn to Pd of 1:1 resulted in the highest overall performance for particles of similar sizes [69, 70]. For the aforementioned PdSn/C results, the current density increased 2- to 2.3-fold at 0.4 V vs. RHE. During constant potential holds, the Pd/C has a continued decrease, while the PdSn/C alloys stabilize after 500 s [70].

Alloying bismuth (Bi) with Pd/C has resulted in a slight decrease in performance but an increase in stability during a constant DFAFC operation at 0.3 V (Fig. 4.7) [71]. Unfortunately after 2 h of continued operation, the performance of PdBi/C

Table 4.3 Activity of extended surface intermetallics, from anodic portion of cyclic voltammogram in 0.125 M formic acid and 0.1 M $HClO_4$ (except Pt_3Sn and PtSb in 0.25 M formic acid) at 10 mV s^{-1}

Electrode	Onset *E* (V)	Anode peak *E* (V)	Anode peak *I* (mA cm^{-1})
Pt	0.317	0.847	0.5
PtBi	0.357	0.752	3.8
PtIn	0.247	0.697	0.93
Pt_3Sn	0.297	0.577	0.35
Pt_2Sn_3		0.627	0.02
PtSb	0.197	0.457	0.1

Potentials (*E*) vs. RHE and current (*I*) (modified from [16])

approached that of Pt/C, while a PtRu/C catalyst had improved activity. The last two catalysts included in Fig. 4.7 are for Sn and Pb adatom-decorated Pt/C, for which Sn only minimally increased activity and Pb had a significant impact, exceeding the performance of Pd with much better performance stability.

4.2.3 Intermetallics

Transformation of alloys into ordered intermetallics through various thermal treatments results in a tuning mechanism of the structural, geometric, and electronic character of the catalyst. The inner atomic bond distances are altered with the addition of a secondary metal.

The DiSalvo group at Cornell University has intensely studied intermetallics for formic acid electrooxidation and observed significant enhancements in turnover efficiencies [16, 46, 72–79]. Table 4.3 compares the activity of several extended intermetallic surfaces in comparison to a Pt baseline [16]. The onset potential relevant to enhanced reactivity through the direct dehydrogenation pathway was most impacted by the addition of Sb. The introduction of both Sn and Sb into the Pt unit cell negatively impacted the anodic peak current. While Bi increased the peak current, it had an adverse impact on the onset potential. It increased the onset potential by 0.06 V and nearly doubled the peak current. The key challenges related to intermetallics for DFAFCs are surfactant-free synthesis methods and reduced nanoparticle sizes (>10 nm) to improve mass activity of the catalyst [74, 75, 80]. Mastumoto et al. compared the mass activity of PtPb 10–20 nm intermetallic particles to a commercial nanocatalyst [79]. During a 9 h hold at 0.197 V vs. RHE, the PtPb intermetallic catalyst demonstrated over a twofold sustained mass activity over that of Pd.

4.3 Catalyst Supports

There have been a number of recent reviews of supports for fuel cell catalysts [12, 13, 81]. Although these focus on oxygen reduction and methanol oxidation, they provide an excellent overview of the breadth of support materials that are available, mechanistic information, and include some examples for formic acid oxidation. Various types of high surface area carbons have been most commonly used as supports for formic acid oxidation catalysts. However, there is now growing interest in the use of various metals, metal oxides, and conducting polymers.

Several studies have been performed on alternative extended carbon support structures: Pd/graphite rods [82], Pd/nanotubes [83], and Pd/nanofibers [84]. However, it is difficult to distinguish between catalyst size and atomic structure differences. Zhang et al. attributed the performance enhancements to an increase in the relative abundance of the more active Pd(111) facet [82].

Iridium alloyed on Pt has been tested on different supports: Pt_xIr_{1-x}/Au [85] and PtIr/Ti [86]. Chen and Chen have demonstrated an initial performance increase for $Pt_{0.5}Ir_{0.5}$/Au, with an average particle size of 2 nm, of 9.4-fold at 0.459 V vs. RHE [85]. Unfortunately, the performance decayed quickly and within 30 min had decreased to a value only twofold higher than that of Pt/C. NanoPtSn/Ti surfaces were prepared resulting in cyclic voltammetric profiles similar to Pt/C [87]. For the aforementioned results, it is difficult to decouple the impacts of metal–support interactions.

The most widely studied conducting polymer support is polyaniline (PANI), which has been shown to decrease the poisoning of Pt by CO_{ads} [88]. Gharibi et al. have recently explored the factors responsible for the enhanced formic acid oxidation activity of Pt supported on a carbon/PANI composite [89]. They concluded that improvements in both electron and proton conductivities, as well as the increased methanol diffusion coefficient and decreased catalyst poisoning, could be involved. A carbon nanotubes/PANI composite [90], poly(*o*-methoxyaniline) [91], and polyindole [92] have recently been reported as effective supports for formic acid oxidation at Pt nanoparticles, while polycarbazole [93] has also been used to support PtRu nanoparticles.

Because of its lower cost relative to Pt, there is growing interest in the development of supported Pd catalysts for formic acid oxidation. Synergies between Pd and PANI supports are well documented [94], while poly(diphenylamine-co-3-aminobenzonitrile) [95] has recently been shown to provide enhanced and more stable activities. Addition of 3-aminobenzonitrile to poly(diphenylamine) was found to improve the dispersion of the Pd, while both polymers eliminated the current decay seen over 1 h for carbon supported Pd.

Pb oxide [96], W oxide [97, 98], and Ce oxide [99] have been shown to notably promote formic acid oxidation at Pt and/or Pd. In the case of Pb oxide, a Pd-Pt-PbO_x/C catalyst was shown to be less susceptible to poisoning than Pd/C, exhibiting a superior performance after ca. 800 s at 0.15 V vs. Ag/AgCl [100].

4.4 Conclusions

Considerable progress has been made in the development of supported Pt-based catalysts for formic acid oxidation, with a variety of Pt alloy, intermetallic, and surface-modified catalysts showing impressive increases in performance relative to Pt/C. The use of Au, Bi, Pb, or Sb as the second metal has been shown to be particularly beneficial, although it is not clear yet whether any of these metals combined with Pt will provide sufficient long-term durability, nor which type of modification of the Pt structure (alloy, intermetallic, or surface modified) is most suitable.

The high cost of Pt continues to be a significant issue. This has been partially addressed by the use of a variety of supports, which allow better dispersion of the Pt in small particles (1–4 nm) with high area/mass ratios. Replacement of a significant fraction of the Pt with a second metal is also an effective way of decreasing the required loading of Pt, as in $Pd_{0.9}Pt_{0.1}$/C, $Pt_{0.5}Au_{0.5}$/C, and the PtPb and PtSb intermetallics.

Improvements in Pd-based catalysts have been modest in comparison with the advances in Pt-based catalysts, although this needs to be considered in the context of the far superior activity of pure Pd over pure Pt. Slow loss of activity, over a period of hours, remains a problem for all Pd-based catalysts, to the point where Pt-based catalysts provide better performances over long time periods.

Future advances in the catalysis of formic acid oxidation will benefit from further development of our understanding of the fundamental processes involved via single crystal and computational studies. Refinement of synthesis methods to produce nanoparticles with the most active and durable geometries and structures will allow fine-tuning of catalysts. Continued discovery of support effects and advances in the understanding of such effects will create additional opportunities to improve performances, lower costs, and enhance durability.

References

1. Arenz M, Stamenkovic V, Schmidt TJ, Wandelt K, Ross PN, Markovic NM (2003) The electro-oxidation of formic acid on Pt–Pd single crystal bimetallic surfaces. Phys Chem Chem Phys 5:4242–4251
2. Peng B, Wang H-F, Liu Z-P, Cai W-B (2010) Combined surface-enhanced infrared spectroscopy and first-principles study on electro-oxidation of formic acid at Sb-modified Pt electrodes. J Phys Chem C 114:3102–3107
3. Wang H-F, Liu Z-P (2009) Formic acid oxidation at Pt/H_2O interface from periodic DFT calculations integrated with a continuum solvation model. J Phys Chem C 113:17502–17508
4. Luo Q, Feng G, Beller M, Jiao H (2012) Formic acid dehydrogenation on Ni(111) and comparison with Pd(111) and Pt(111). J Phys Chem C 116:4149–4156
5. Llorca MJ, Feliu JM, Aldaz A, Clavilier J (1994) Formic acid oxidation on Pdad + Pt(100) and Pdad + Pt(111) electrodes. J Electroanal Chem 376:151–160

6. Babu PK, Kim HS, Chung JH, Oldfield E, Wieckowski A (2004) Bonding and motional aspects of CO adsorbed on the surface of Pt nanoparticles decorated with Pd. J Phys Chem B 108:20228–20232
7. Baldauf M, Kolb DM (1996) Formic acid oxidation on ultrathin Pd films on Au(hlk) and Pt (hkl) electrodes. J Phys Chem 100:11375–11381
8. Pan Y, Zhang R, Blair SL (2009) Anode poisoning study in direct formic acid fuel cells. Electrochem Solid St Lett 12:B23–B26
9. Solla-Gullon J, Montiel V, Aldaz A, Clavilier J (2002) Electrochemical and electrocatalytic behavior of platinum–palladium nanoparticle alloys. Electrochem Commun 4:716–721
10. Hartley FR (1991) The occurrence, extraction, properties and uses of the platinum group metals in studies in inorganic chemistry. In: Hartley FR (ed) Chemistry of the platinum group metals: recent developments, vol 11. Elsevier, Amsterdam, p 642
11. Uhm S, Lee HJ, Lee J (2009) Understanding underlying processes in formic acid fuel cells. Phys Chem Chem Phys 11:9326–9336
12. Wang Y-J, Wilkinson DP, Zhang J (2011) Non-carbon support materials for polymer electrolyte membrane fuel cell electrocatalysts. Chem Rev 111:7625–7651
13. Sharma S, Pollet BG (2012) Support materials for PEMFC and DMFC electrocatalysts-A review. J Power Sources 208:96–119
14. Park S, Xie Y, Weaver MJ (2002) Electrocatalytic pathways on carbon-supported platinum nanoparticles: comparison of particle-size-dependent rates of methanol, formic acid, and formaldehyde electrooxidation. Langmuir 18:5792–5798
15. Zhou WP, Lewera A, Larsen R, Masel RI, Bagus PS, Wieckowski A (2006) Size effects in electronic and catalytic properties of unsupported palladium nanoparticles in electrooxidation of formic acid. J Phys Chem B 110:13393–13398
16. Casado-Rivera E, Volpe DJ, Alden L, Lind C, Downie C, Vazquez-Alvarez T, Angelo ACD, DiSalvo FJ, Abruna HD (2004) Electrocatalytic activity of ordered intermetallic phases for fuel cell applications. J Am Chem Soc 126:4043–4049
17. Parsons R, VanderNoot T (1988) The oxidation of small organic molecules: a survey of recent fuel cell related research. J Electroanal Chem Interfacial Electrochem 257:9–45
18. Chen Q-S, Zhou Z-Y, Vidal-Iglesias FJ, Solla-Gullon J, Feliu JM, Sun S-G (2011) Significantly enhancing catalytic activity of tetrahexahedral Pt nanocrystals by Bi adatom decoration. J Am Chem Soc 133:12930–12933
19. Clavilier J, Femandez-Vega A, Feliu JM, Aldaz A (1989) Heterogeneous electrocatalysis on well-defined platinum surfaces modified by controlled amounts of irreversibly adsorbed adatoms: Part III. Formic acid oxidation on the Pt (100)–Bi system. J Electroanal Chem Interfacial Electrochem 261:113–125
20. Clavilier J, Fernandez-Vega A, Feliu JM, Aldaz A (1989) Heterogeneous electrocatalysis on well defined platinum surfaces modified by controlled amounts of irreversibly adsorbed adatoms: Part I. Formic acid oxidation on the Pt (111)–Bi system. J Electroanal Chem Interfacial Electrochem 258:89–100
21. Daniele S, Bergamin S (2007) Preparation and voltammetric characterisation of bismuth-modified mesoporous platinum microelectrodes. Application to the electrooxidation of formic acid. Electrochem Commun 9:1388–1393
22. Herrero E, Feliu JM, Aldaz A (1994) Poison formation reaction from formic acid on Pt(100) electrodes modified by irreversibly adsorbed bismuth and antimony. J Electroanal Chem 368:101–108
23. Kang S, Lee J, Lee JK, Chung S-Y, Tak Y (2006) Influence of Bi modification of Pt anode catalyst in direct formic acid fuel cells. J Phys Chem B 110:7270–7274
24. Kim B-J, Kwon K, Rhee CK, Han J, Lim T-H (2008) Modification of Pt nanoelectrodes dispersed on carbon support using irreversible adsorption of Bi to enhance formic acid oxidation. Electrochim Acta 53:7744–7750
25. Maciá MD, Herrero E, Feliu JM (2003) Formic acid oxidation on Bi–Pt(1 1 1) electrode in perchloric acid media. A kinetic study. J Electroanal Chem 554–555:25–34

26. Saez A, Exposito E, Solla-Gullon J, Montiel V, Aldaz A (2012) Bismuth-modified carbon supported Pt nanoparticles as electrocatalysts for direct formic acid fuel cells. Electrochim Acta 63:105–111
27. Yu X, Pickup PG (2011) Carbon supported PtBi catalysts for direct formic acid fuel cells. Electrochim Acta 56:4037–4043
28. Bauskar A, Rice CA (2013) Bi modified Pt/C for enhanced formic acid electro-oxidation. Electrochim Acta 93:152–157
29. Yu X, Pickup PG (2010) Pb and Sb modified Pt/C catalysts for direct formic acid fuel cells. Electrochim Acta 55:7354–7361
30. Xia XH, Iwasita T (1993) Influence of underpotential deposited lead upon the oxidation of formic acid in perchloric acid at platinum electrodes. J Electrochem Soc 140:2559–2565
31. Uhm S, Chung ST, Lee J (2007) Activity of Pt anode catalyst modified by underpotential deposited Pb in a direct formic acid fuel cell. Electrochem Commun 9:2027–2031
32. Fernandez-Vega A, Feliu JM, Aldaz A, Clavilier J (1989) Heterogeneous electrocatalysis on well defined platinum surfaces modified by controlled amounts of irreversibly adsorbed adatoms: Part II. Formic acid oxidation on the Pt (100)-Sb system. J Electroanal Chem Interfacial Electrochem 258:101–113
33. Lee JK, Jeon H, Uhm S, Lee J (2008) Influence of underpotentially deposited Sb onto Pt anode surface on the performance of direct formic acid fuel cells. Electrochim Acta 53:6089–6092
34. Herrero E, Fernández-Vega A, Feliu JM, Aldaz A (1993) Poison formation reaction from formic acid and methanol on Pt(111) electrodes modified by irreversibly adsorbed Bi and As. J Electroanal Chem 350:73–88
35. Fernandez-Vega A, Feliu JM, Aldaz A, Clavilier J (1991) Heterogeneous electrocatalysis on well-defined platinum surfaces modified by controlled amounts of irreversibly adsorbed adatoms: Part IV. Formic acid oxidation on the Pt(111)–As system. J Electroanal Chem Interfacial Electrochem 305:229–240
36. Bi X, Wang R, Ding Y (2011) Boosting the performance of Pt electro-catalysts toward formic acid electro-oxidation by depositing sub-monolayer Au clusters. Electrochim Acta 56:10039–10043
37. Herrero E, Llorca MJ, Feliu JM, Aldaz A (1995) Oxidation of formic acid on Pt(100) electrodes modified by irreversibly adsorbed tellurium. J Electroanal Chem 383:145–154
38. Herrero E, Llorca MJ, Feliu JM, Aldaz A (1995) Oxidation of formic acid on Pt(111) electrodes modified by irreversibly adsorbed tellurium. J Electroanal Chem 394:161–167
39. Llorca MJ, Herrero E, Feliu JM, Aldaz A (1994) Formic acid oxidation on Pt(111) electrodes modified by irreversibly adsorbed selenium. J Electroanal Chem 373:217–225
40. Rice C, Ha S, Masel RI, Wieckowski A (2003) Catalysts for direct formic acid fuel cells. J Power Sources 115:229–235
41. Waszczuk P, Barnard TM, Rice C, Masel RI, Wieckowski A (2002) A nanoparticle catalyst with superior activity for electrooxidation of formic acid. Electrochem Commun 4:732
42. Feliu JM, Herrero E (2010) Formic acid oxidation. In: Vielstich W, Lamm A, Gasteiger HA (eds) Handbook of fuel cells—fundamentals, technology and applications. Wiley, Chichester
43. Neurock M, Janik M, Wieckowski A (2008) A first principles comparison of the mechanism and site requirements for the electrocatalytic oxidation of methanol and formic acid over Pt. Faraday Discuss 140:363–378
44. Leiva E, Iwasita T, Herrero E, Feliu JM (1997) Effect of adatoms in the electrocatalysis of HCOOH oxidation. A theoretical model. Langmuir 13:6287–6293
45. Yu X, Pickup PG (2008) Recent advances in direct formic acid fuel cells (DFAFC). J Power Sources 182:124–132
46. Ghosh T, Zhou Q, Gregoire JM, van Dover RB, DiSalvo FJ (2010) Pt−Cd and Pt−Hg phases as high activity catalysts for methanol and formic acid oxidation. J Phys Chem C 114:12545–12553

47. Yang H, Dai L, Xu D, Fang J, Zou S (2010) Electrooxidation of methanol and formic acid on PtCu nanoparticles. Electrochim Acta 55:8000–8004
48. Abe H, Matsumoto F, Alden LR, Warren SC, Abruña HD, DiSalvo FJ (2008) Electrocatalytic performance of fuel oxidation by Pt3Ti nanoparticles. J Am Chem Soc 130:5452–5458
49. Chen W, Kim J, Sun S, Chen S (2007) Composition effects of FePt alloy nanoparticles on the electro-oxidation of formic acid. Langmuir 23:11303–11310
50. Huang Y, Zheng S, Lin X, Su L, Guo Y (2012) Microwave synthesis and electrochemical performance of a PtPb alloy catalyst for methanol and formic acid oxidation. Electrochim Acta 63:346–353
51. Liu Z, Guo B, Tay SW, Hong L, Zhang X (2008) Physical and electrochemical characterizations of PtPb/C catalyst prepared by pyrolysis of platinum(II) and lead(II) acetylacetonate. J Power Sources 184:16–22
52. Obradovic MD, Rogan JR, Babic BM, Tripkovic AV, Gautam ARS, Radmilovic VR, Gojkovic SL (2012) Formic acid oxidation on Pt–Au nanoparticles: relation between the catalyst activity and the poisoning rate. J Power Sources 197:72–79
53. Chen G, Li Y, Wang D, Zheng L, You G, Zhong C-J, Yang L, Cai F, Cai J, Chen BH (2011) Carbon-supported PtAu alloy nanoparticle catalysts for enhanced electrocatalytic oxidation of formic acid. J Power Sources 196:8323–8330
54. Yu X, Pickup PG (2011) Codeposited PtSb/C catalysts for direct formic acid fuel cells. J Power Sources 196:7951–7956
55. Zhang H-X, Wang C, Wang J-Y, Zhai J-J, Cai W-B (2010) Carbon-supported Pd–Pt nanoalloy with low Pt content and superior catalysis for formic acid electro-oxidation. J Phys Chem C 114:6446–6451
56. Feng L, Si F, Yao S, Cai W, Xing W, Liu C (2011) Effect of deposition sequences on electrocatalytic properties of PtPd/C catalysts for formic acid electrooxidation. Catal Commun 12:772–775
57. Li X, Hsing IM (2006) Electrooxidation of formic acid on carbon supported Pt_xPd_{1-x} (x=0–1) nanocatalysts. Electrochim Acta 51:3477–3483
58. Wang J-Y, Kang Y-Y, Yang H, Cai W-B (2009) Boron-doped palladium nanoparticles on carbon black as a superior catalyst for formic acid electro-oxidation. J Phys Chem C 113:8366–8372
59. Sun H, Xu J, Fu G, Mao X, Zhang L, Chen Y, Zhou Y, Lu T, Tang Y (2012) Preparation of highly dispersed palladium-phosphorus nanoparticles and its electrocatalytic performance for formic acid electrooxidation. Electrochim Acta 59:279–283
60. Yang G, Chen Y, Zhou Y, Tang Y, Lu T (2010) Preparation of carbon supported Pd–P catalyst with high content of element phosphorus and its electrocatalytic performance for formic acid oxidation. Electrochem Commun 12:492–495
61. Zhang L, Tang Y, Bao J, Lu T, Li C (2006) A carbon-supported Pd–P catalyst as the anodic catalyst in a direct formic acid fuel cell. J Power Sources 162:177–179
62. Mazumder V, Chi M, Mankin MN, Liu Y, Metin O, Sun D, More KL, Sun S (2012) A facile synthesis of MPd (M = Co, Cu) nanoparticles and their catalysis for formic acid oxidation. Nano Lett 12:1102–1106
63. Morales-Acosta D, Ledesma-Garcia J, Godinez LA, Rodriguez HG, Alvarez-Contreras L, Arriaga LG (2010) Development of Pd and Pd–Co catalysts supported on multi-walled carbon nanotubes for formic acid oxidation. J Power Sources 195:461–465
64. Sangarunlert W, Sukchai S, Pongtornkulpanich A, Nathakaranakule A, Luschtinetz T (2011) Technical and economic evaluation of a formic acid/hydrogen peroxide fuel cell system with Pt-M/C as anode catalyst. J Fuel Cell Sci Technol 8:061005–061007
65. Wang R, Liao S, Ji S (2008) High performance Pd-based catalysts for oxidation of formic acid. J Power Sources 180:205–208
66. Wang X, Xia Y (2008) Electrocatalytic performance of PdCo-C catalyst for formic acid oxidation. Electrochem Commun 10:1644–1646

67. Habibi B, Delnavaz N (2012) Electrosynthesis, characterization and electrocatalytic properties of Pt–Sn/CCE towards oxidation of formic acid. RSC Adv 2:1609–1617
68. DandanTu WB, Wang B, Deng C, Gao Y (2011) A highly active carbon-supported PdSn catalyst for formic acid electrooxidation. Appl Catal B 103:163–168
69. Zhang Z, Ge J, Ma L, Liao J, Lu T, Xing W (2009) Highly active carbon-supported PdSn catalysts for formic acid electrooxidation. Fuel Cells 9:114–120
70. Liu Z, Zhang X (2009) Carbon-supported PdSn nanoparticles as catalysts for formic acid oxidation. Electrochem Commun 11:1667–1670
71. Yu X, Pickup PG (2011) Screening of PdM and PtM catalysts in a multi-anode direct formic acid fuel cell. J Appl Electrochem 41:589–597
72. Alden LR, Han DK, Matsumoto F, Abruna HD, DiSalvo FJ (2006) Intermetallic PtPb nanoparticles prepared by sodium naphthalide reduction of metal-organic precursors: electrocatalytic oxidation of formic acid. Chem Mater 18:5591–5596
73. Casado-Rivera E, Gal Z, Angelo ACD, Lind C, DiSalvo FJ, Abruna HD (2003) Electrocatalytic oxidation of formic acid at an ordered intermetallic PtBi surface. Chemphyschem 4:193–199
74. Ghosh T, Leonard BM, Zhou Q, DiSalvo FJ (2010) Pt alloy and intermetallic phases with V, Cr, Mn, Ni, and Cu: synthesis as nanomaterials and possible applications as fuel cell catalysts. Chem Mater 22:2190–2202
75. Leonard BM, Zhou Q, Wu D, DiSalvo FJ (2011) Facile synthesis of PtNi intermetallic nanoparticles: influence of reducing agent and precursors on electrocatalytic activity. Chem Mater 23:1136–1146
76. Liu Y, Lowe MA, DiSalvo FJ, Abruna HD (2010) Kinetic stabilization of ordered intermetallic phases as fuel cell anode materials. J Phys Chem C 114:14929–14938
77. Roychowdhury C, Matsumoto F, Zeldovich VB, Warren SC, Mutolo PF, Ballesteros M, Wiesner U, Abruña HD, DiSalvo FJ (2006) Synthesis, characterization, and electrocatalytic activity of PtBi and PtPb nanoparticles prepared by borohydride reduction in methanol. Chem Mater 18:3365–3372
78. Volpe D, Casado-Rivera E, Alden L, Lind C, Hagerdon K, Downie C, Korzeniewski C, DiSalvo FJ, Abruna HD (2004) Surface treatment effects on the electrocatalytic activity and characterization of intermetallic phases. J Electrochem Soc 151:A971–A977
79. Matsumoto F, Roychowdhury C, DiSalvo FJ, Abruna HD (2008) Electrocatalytic activity of ordered intermetallic PtPb nanoparticles prepared by borohydride reduction toward formic acid oxidation. J Electrochem Soc 155:B148–B154
80. Li X, An L, Wang X, Li F, Zou R, Xia D (2012) Supported sub-5 nm Pt–Fe intermetallic compounds for electrocatalytic application. J Mater Chem 22:6047–6052
81. Antolini E (2010) Composite materials: an emerging class of fuel cell catalyst supports. Appl Catal B 100:413–426
82. Zhang B, Ye D, Li J, Zhu X, Liao Q (2012) Electrodeposition of Pd catalyst layer on graphite rod electrodes for direct formic acid oxidation. J Power Sources 214:277–284
83. Morgan RD, Salehi-khojin A, Masel RI (2011) Superior formic acid oxidation using carbon nanotube-supported palladium catalysts. J Phys Chem C 115:19413–19418
84. Qin Y-H, Jia Y-B, Jiang Y, Niu D-F, Zhang X-S, Zhou X-G, Niu L, Yuan W-K (2012) Controllable synthesis of carbon nanofiber supported Pd catalyst for formic acid electrooxidation. Int J Hydrogen Energy 37:7373–7377
85. Chen W, Chen S (2011) Iridium–platinum alloy nanoparticles: composition-dependent electrocatalytic activity for formic acid oxidation. J Mater Chem 21:9169–9178
86. Yi Q, Chen A, Huang W, Zhang J, Liu X, Xu G, Zhou Z (2007) Titanium-supported nanoporous bimetallic Pt–Ir electrocatalysts for formic acid oxidation. Electrochem Commun 9:1513–1518
87. Yi Q, Zhang J, Chen A, Liu X, Xu G, Zhou Z (2008) Activity of a novel titanium-supported bimetallic PtSn/Ti electrode for electrocatalytic oxidation of formic acid and methanol. J Appl Electrochem 38:695–701

88. Laborde H, Leger JM, Lamy C (1994) Electrocatalytic oxidation of methanol and C1 molecules on highly dispersed electrodes. Part 1. Platinum in polyaniline. J Appl Electrochem 24:219–226
89. Gharibi H, Kakaei K, Zhiani M (2010) Platinum nanoparticles supported by a Vulcan XC-72 and PANI doped with trifluoromethane sulfonic acid substrate as a new electrocatalyst for direct methanol fuel cells. J Phys Chem C 114:5233–5240
90. Shi J, Zhang Z-Y, Hu Y-Q, Hua Y-X (2010) Incorporation of 4-aminobenzene functionalized multi-walled carbon nanotubes in polyaniline for application in formic acid electrooxidation. J Appl Polym Sci 118:1815–1820
91. Ren F, Zhou W, Du Y, Yang P, Wang C, Xu J (2011) High efficient electrocatalytic oxidation of formic acid at Pt dispersed on porous poly(o-methoxyaniline). Int J Hydrogen Energy 36:6414–6421
92. Zhou W, Wang C, Xu J, Du Y, Yang P (2011) High efficient electrooxidation of formic acid at a novel Pt-indole composite catalyst prepared by electrochemical self-assembly. J Power Sources 196:1118–1122
93. Zhou W, Xu J, Du Y, Yang P (2011) Polycarbazole as an efficient promoter for electrocatalytic oxidation of formic acid on Pt and Pt-Ru nanoparticles. Int J Hydrogen Energy 36:1903–1912
94. Moghaddam RB, Pickup PG (2011) Support effects on the oxidation of formic acid at Pd nanoparticles. Electrocatalysis 2:159–162
95. Philips MF, Gopalan AI, Lee K-P (2011) Enhanced electrocatalytic performance of cyano groups containing conducting polymer supported catalyst for oxidation of formic acid. Catal Commun 12:1084–1087
96. Buzzo GS, Niquirilo RV, Suffredini HB (2010) Active Pt–PbO_x/C anodes to promote the formic acid oxidation in presence of sulfuric acid. J Braz Chem Soc 21:185–190
97. Zhang Z, Huang Y, Ge J, Liu C, Lu T, Xing W (2008) WO_3/C hybrid material as a highly active catalyst support for formic acid electrooxidation. Electrochem Commun 10:1113–1116
98. Feng L-G, Yan L, Cui Z-M, Liu C-P, Xing W (2011) High activity of Pd–WO_3/C catalyst as anodic catalyst for direct formic acid fuel cell. J Power Sources 196:2469–2474
99. Wang Y, Wang S, Wang X (2009) CeO_2 promoted electrooxidation of formic acid on Pd/C nano-electrocatalysts. Electrochem Solid-State Lett 12:B73–B76
100. Niquirilo RV, Teixeira-Neto E, Buzzo GS, Suffredini HB (2010) Formic acid oxidation at Pd, Pt and PbO_x-based catalysts and calculation of their approximate electrochemical active areas. Int J Electrochem Sci 5:344–354
101. Liu Z, Hong L, Tham MP, Lim TH, Jiang H (2006) Nanostructured Pt/C and Pd/C catalysts for direct formic acid fuel cells. J Power Sources 161:831–835
102. Markovic NM, Schmidt TJ, Stamenkovic V, Ross PN (2001) Oxygen reduction reaction on Pt and Pt bimetallic surfaces: a selective review. Fuel Cells 2:105